APL Materials

Efficient and affordable thermomagnetic materials for harvesting low grade waste heat

Daniel Dzekan, Anja Waske, Kornelius Nielsch, and Sebastian Fähler

View Online   Export Citation   CrossMark

ARTICLES YOU MAY BE INTERESTED IN

AIP Publishing

Efficient and affordable thermomagnetic materials for harvesting low grade waste heat

View Online   Export Citation   CrossMark

Daniel Dzekan,[1,2] (iD) **Anja Waske,**[3] **Kornelius Nielsch,**[1,2] (iD) and **Sebastian Fähler**[1,a] (iD)

AFFILIATIONS

[1] Leibniz IFW Dresden, Helmholtzstraße 20, Dresden 01069, Germany
[2] TU Dresden, Institut für Werkstoffwissenschaft, Helmholtzstraße 7, Dresden 01069, Germany
[3] Bundesanstalt für Materialforschung und –prüfung (BAM), Unter den Eichen 87, Berlin 12205, Germany

[a] Author to whom correspondence should be addressed: s.faehler@ifw-dresden.de

ABSTRACT

Industrial processes release substantial quantities of waste heat, which can be harvested to generate electricity. At present, the conversion of low grade waste heat to electricity relies solely on thermoelectric materials, but such materials are expensive and have low thermodynamic efficiencies. Although thermomagnetic materials may offer a promising alternative, their performance remains to be evaluated, thereby hindering their real-world application. Here, the efficiency and cost effectiveness of thermomagnetic materials are evaluated for the usage in motors, oscillators, and generators for converting waste heat to electricity. The analysis reveals that up to temperature differences of several 10 K, the best thermomagnetic materials have the potential to compete with thermoelectric materials. Importantly, it is found that the price per watt of some thermomagnetic materials is much lower compared to that of present-day thermoelectrics, which can become competitive with conventional power plants. This materials library enables the selection of the best available thermomagnetic materials for harvesting waste heat and gives guidelines for their future development.

I. INTRODUCTION

Humanity finds itself at a tipping point at which the efficient use of primary energy has become decisive.[1] An important option in this regard is to recover waste heat, which is released during industrial and chemical processes in a quantity that is equivalent to almost 72% of all electrical energy produced in 2016.[2] However, most of the waste heat is just above room temperature,[3] at which few existing technologies can convert heat to electricity. Although thermoelectric generators can work in this temperature range, they suffer from low thermodynamic efficiency and high price.[4,5] Thus, there is a strong need for alternative energy materials for the conversion of low grade waste heat to electricity.

Magnetic materials have an outstanding position within the class of energy materials. The combination of hard and soft magnetic materials in electric motors and generators is the state of the art for the conversion of electrical energy to mechanical energy, and vice versa. Magnetocaloric materials expand the application range further toward the conversion of electrical energy to thermal energy.[6,7] In these materials, a steep change in magnetization around room temperature yields a magnetically induced entropy change, which drives a highly efficient magnetocaloric cooling cycle.[8] Intense research on magnetocaloric materials[9] has led to the development of several devices and prototypes[10] that enable energy efficient cooling. The rapid progress in magnetocaloric materials has also opened up the possibility of the reverse process: converting thermal energy to electrical energy in thermomagnetic systems. Although the first concepts for thermomagnetic energy harvesting had been already suggested by Tesla,[11,12] Stefan,[13] and Edison[14,15] more than 100 years ago, it required the development of magnetocaloric materials to build the first thermomagnetic demonstrators.[16]

In this paper, we introduce thermomagnetic materials (TMMs) as dedicated energy materials for harvesting waste heat. To identify the differences from magnetocaloric materials, we analyze the thermomagnetic harvesting cycle and describe how this cycle is implemented within thermomagnetic motors, oscillators, and generators. From this, we derive generalized criteria for the magnetic and thermal properties required for optimum thermodynamic efficiency and

cost effectiveness. We use these criteria to benchmark thermomagnetic materials in two Ashby plots as figures of merit and predict guidelines for their development. From our materials library, we analyze the four most promising TMMs and specify their application areas. For harvesting low grade waste heat, we identify La–Fe–Co–Si as the best TMM available today, which can compete with thermoelectric materials with respect to both thermodynamic efficiency and cost effectiveness.

II. EXPERIMENTAL SECTION

For our materials library, we digitized material data from their primary sources, and all data are listed in Table S1 of the supplementary material. For our analysis, we selected a symmetric temperature span $\Delta T = T_{\text{hot}} - T_{\text{cold}}$ between the hot and cold temperatures around the transition temperature T_t. The magnetization difference was derived from temperature-dependent measurements at sufficient magnetic fields or from field-dependent measurements at 1 T. The energy input in the form of heat to achieve this magnetization change is determined by the heat capacity of the material. We took heat capacity data from zero-field measurements. The heat capacity was calculated as the mean value for $\Delta T = 30$ K. The digitized data were integrated to calculate the magnetic energy and the heat input. The precise determination of magnetic energy and heat input is given exemplarily for La–Fe–Co–Si in Figs. S1 and S2 of the supplementary material.

Based on the thermodynamic cycle, described later in detail, we evaluate the power output as one decisive property of a thermomagnetic material. For the calculation, it is necessary to calculate a time at which the temperature and, thus, magnetization of the material can change. Therefore, we used the lumped capacitance method, which is described in Fig. S7 of the supplementary material. To evaluate this equation, heat conductivity and mass density are required, which were taken from their primary sources in the vicinity of the transition temperature. Relating the power output to the materials cost results in the cost effectiveness of this particular material. For this economic consideration, we compiled the raw material costs from different material marketplaces, as given in Table S1 of the supplementary material.

III. RESULTS AND DISCUSSION

A. The thermomagnetic cycle for harvesting waste heat

To identify the requirements for high thermodynamic efficiency of thermomagnetic materials (TMMs), we first describe a thermomagnetic cycle [Fig. 1(a)] and then identify the differences compared to a magnetocaloric cooling cycle. This generalized approach is based on equilibrium thermodynamics and allows treating all thermomagnetic harvesting devices together, analyzed in Sec. III B. Within a thermomagnetic cycle, the TMM is used as the functional material, which reduces its magnetization M at a transition temperature T_t. Step I starts at ambient temperature, where the TMM is below T_t and exhibits a high M_{cold}. At constant temperature, a magnetic field H is applied, which reduces the Gibbs energy of the TMM by $-\mu_0 M_{\text{cold}} H$, where μ_0 is the magnetic field constant.[17] In step II, low grade waste heat Q_{in} is used to heat the TMM above T_t, which reduces magnetization to M_{hot}. When the magnetic field is

removed in step III, just a low value of Gibbs energy term $+\mu_0 M_{\text{hot}} H$ is required.

In step IV, the hot TMM is brought again into contact with ambient temperature, which closes the thermomagnetic cycle and restores the high M_{cold}. The difference in Gibbs energy $-\mu_0 \Delta M H$ is used to create electrical energy, with $\Delta M = M_{\text{cold}} - M_{\text{hot}}$ being the decisive material property. As this contribution to Gibbs energy only contains magnetic properties, we call the positive counterpart, which is harvested by thermomagnetic systems, as magnetic energy (density),

$$E_M = +\mu_0 \Delta M H, \qquad (1)$$

and drop the term "density" for better readability. During one cycle, the TMM converts E_M; thus, a thermomagnetic system can at best convert E_M to electrical energy.

A thermomagnetic cycle follows an Ericcson cycle, which differs from a magnetocaloric (Carnot) cycle in two aspects. First, a thermomagnetic cycle consists of two isothermal and two isofield steps, whereas, in a conventional magnetocaloric cycle, the isothermal steps are replaced by adiabatic ones.[8] Only in rare cases, an Ericcson cycle was used for refrigeration.[18] Second, Q_{in} is the thermal input energy and E_M is the output energy, which are vice versa within a magnetocaloric cycle. Both aspects have impact on efficiency and are treated in detail later.

B. Thermomagnetic motors, oscillators, and generators

The thermodynamic cycle is implemented in several thermomagnetic devices, and we introduce a classification depending on the type of mechanical movement involved. As a comprehensive collection of devices had recently been given by Kishore and Priya,[19] as well as Kitanovski,[20] here we show that, despite these different movements, the TMM is always subjected to the same thermomagnetic cycle.

Mechanical rotation is employed within a thermomagnetic motor [Fig. 1(b)]. First proposals of such devices were made by Edison,[14] Tesla,[11] and Stefan,[13] and later works predicted the efficiency of such a device to reach the thermodynamic limit.[21–23] A thermomagnetic motor uses a rotatable ring of TMM. Its rotation causes each part of the TMM to undergo the four stages of the thermodynamic cycle. In stage I, the application of a magnetic field H is realized by a permanent magnet. As the TMM exhibits a high M_{cold}, it is strongly attracted by the field gradient at the edge of the permanent magnet. The integral gain of mechanical energy associated with this torque is identical to $\mu_0 M_{\text{cold}} H$. In stage II, the TMM is heated by the low grade waste heat, which reduces the magnetization to M_{hot}. Thus, when the TMM leaves the permanent magnet region in stage III, only a low torque hinders the rotation of the TMM ring. In step IV, the temperature of the TMM reduces to ambient and restores the high M_{cold}. Thus, in a thermomagnetic motor, the heat Q_{in} is used to convert the magnetic energy $E_M = \mu_0 \Delta M H$ into mechanical energy, which can be converted to electrical energy by a conventional generator. Although many miniature versions of this motor, known also as the "Curie wheel," can be viewed on video-sharing websites, these motors can also be more powerful, e.g., a prototype using gadolinium as the TMM reached a power of 1.4 kW.[24]

Mechanical oscillation is used within thermomagnetic microsystems. In these systems, the TMM is used in the shape of
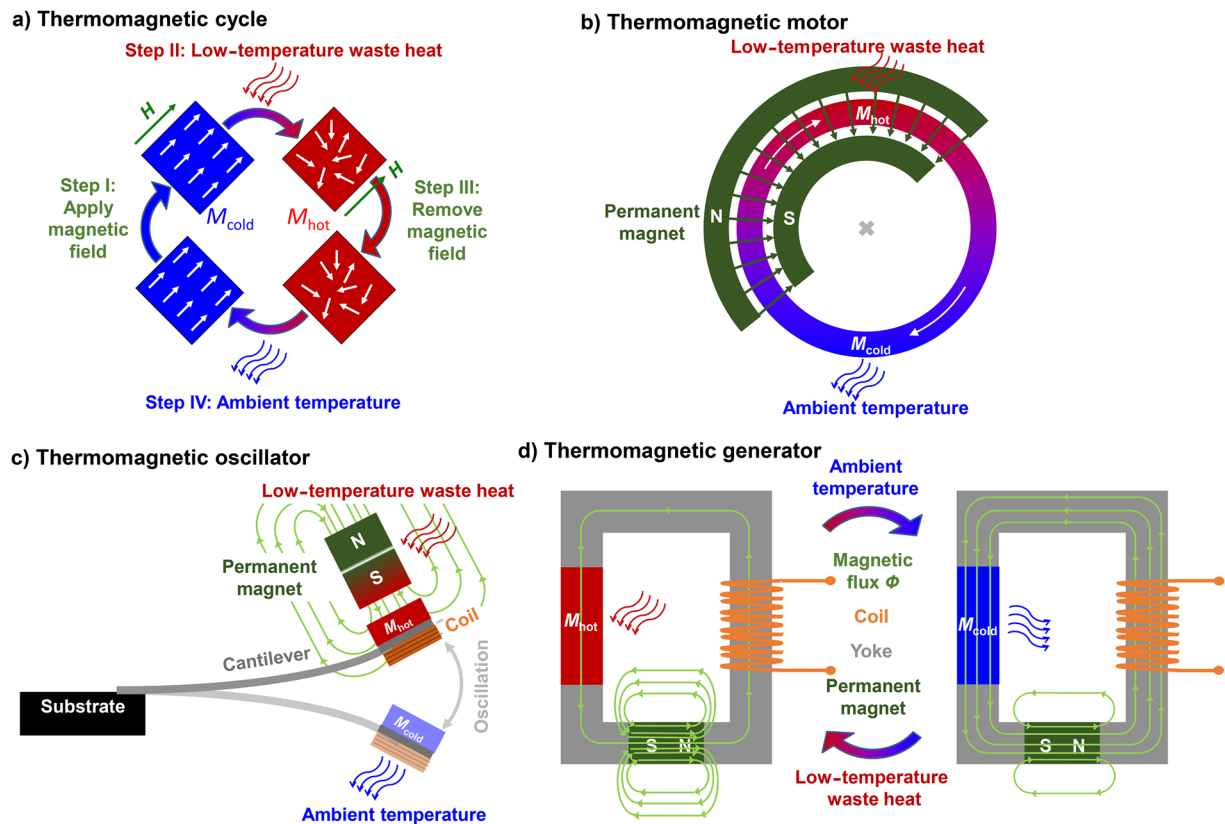
FIG. 1. Thermomagnetic harvesting of low-temperature waste heat. (a) A thermomagnetic material (TMM) is subjected to four steps within a thermomagnetic cycle. In step I, a magnetic field H is applied to the cold TMM (blue) that has a high magnetization M_{cold}, which increases its Gibbs energy. In step II, low grade waste heat Q_{in} is used to increase the temperature of the TMM (red), which reduces its magnetization to M_{hot}. Thus, when the magnetic field is removed in step III, there is just a low increase in Gibbs energy. In step IV, the TMM is cooled to ambient, which restores its high magnetization M_{cold} and closes the thermomagnetic cycle. The difference in Gibbs energy can be harvested by one of the following setups. (b) A rotatable ring of TMM (blue–red color gradient according to its temperature) in a thermomagnetic motor is subjected to the thermomagnetic cycle. (c) A TMM film is mounted at the tip of a cantilever within a thermomagnetic oscillator. An additional induction coil at the tip of the cantilever converts the mechanical oscillation within the gradient of the permanent magnet to electric energy. (d) The TMM within a thermomagnetic generator is used to switch the magnetic flux Φ (green arrows) within a magnetic circuit during cycling between hot (left) and cold (right). In this circuit, Φ is created by a permanent magnet (green) and guided by a soft magnetic yoke (gray). As the magnetic field acting on the TMM changes with the flux, a thermomagnetic generator is, thus, an implementation of a four step thermomagnetic cycle.

a thin film deposited on top of a vibrating cantilever [Fig. 1(c)]. In step I of the thermomagnetic cycle, the cold TMM film is attracted by a permanent magnet, which bends the cantilever. The permanent magnet is combined with the heat source, and thus, in step II, the temperature of the TMM increases, which reduces its magnetization. This decreases the attractive force of the TMM toward the permanent magnet. Accordingly, in step III, the restoring force of the bent cantilever is sufficient to move the TMM away from the heat source. With the heat source also being the permanent magnet, H is reduced. At sufficient distance, the TMM cools to ambient (step IV). The mechanical energy of the vibrating cantilever is converted to electrical energy by an induction coil, which is located on top of the cantilever.[25] During vibration, this coil moves within the magnetic field gradient of the permanent magnet, and thus, according to Faraday's law of induction, the flux change induces an electric voltage. In a different design,[26] as suggested by the group

of Carman,[27–29] a piezoelectric cantilever is used instead of the coil. Although bulk thermomagnetic oscillators, which act like a linear motor, have also been demonstrated,[30] the advantage of a microsystem is its fast heat exchange, which is possible because of the reduced size of the TMM. This results in a high frequency of the thermomagnetic cycle, which can reach up to 200 Hz when the resonance frequency of the cantilever matches the thermal exchange frequency.[25]

No mechanical movement of the TMM is required for a thermomagnetic generator. First concepts of generators were invented by Edison[15] and Tesla,[12] and later, Brillouin and Iskenderian calculated the efficiency relative to Carnot to be up to 55%.[31] Based on this work, other researchers treated such a device theoretically.[32–35] In this implementation of a thermomagnetic cycle, the TMM is used as a thermal switch for the magnetic flux Φ, which is created by a permanent magnet [Fig. 1(d)]. At low temperatures, the high M_{cold}

of the TMM guides Φ through a closed magnetic circuit. At high temperatures, the low M_{hot} opens the magnetic circuit and reduces Φ. Following Faraday's law of induction, this flux change induces an electric voltage. To harvest electric energy, an induction coil is wound around the soft magnetic yoke, connecting the permanent magnet and TMM. The flux change during steps II and IV converts magnetic energy E_M into electrical energy. Opening and closing the magnetic circuit also changes the magnetic field H that acts on the TMM, as illustrated by the different density of flux lines in Fig. 1(d). The first proof of concept was published by Srivastava *et al.* in 2011.[16] The efficiency of this demonstrator was quite low, mainly because of an unoptimized magnetic circuit. As a large difference in Φ is beneficial to increase E_M, more complex magnetic field topologies have been used for thermomagnetic generators. A topology with two magnetic circuits avoids magnetic stray fields.[36] A topology with three circuits even allows for a sign reversal of Φ, which increases both output voltage and power by orders of magnitude.[37]

C. Efficiency of thermomagnetic materials

Thermodynamic efficiency is a key property of each energy harvesting process as it defines the fraction of usable output energy vs thermal input energy Q_{in} during each cycle. For the TMM, the magnetic energy E_M is the upper limit of the output energy, which gives the material efficiency

$$\eta = \frac{E_M}{Q_{in}} = \frac{\mu_0 \Delta M H}{Q_{in}}. \quad (2)$$

Though this equation is based on the simplification of equilibrium thermodynamics, most implementations today reach even much lower values for the system efficiency.[36,37] Possible reasons for this are thermodynamic cycles that do not consist of strict isothermal/isofield steps, losses by insufficient insulation, which are challenging at low frequencies, or an incomplete use of Q_{in} to heat up the TMM. Here, we focus on the upper limits as defined by material efficiency and do not address the system engineering aspects as we expect a strong improvement from the very few existing prototypes.

For many TMMs, the physical quantities used in Eq. (2) are available and summarized in Table S1 of the supplementary material, since they can be extracted from available measurements, as described in Fig. S2 of the supplementary material. The applied magnetic field H is the only property in the equation that depends on the device and not on the material. To compare material properties, we fix $\mu_0 H = 1$ T, given that a field of 1 T can be easily obtained by currently available permanent magnets. As the minimum field, we used zero, which can be approached well by magnetic shielding as used, e.g., in magnetocaloric devices.[38] To identify the TMM with highest η, we evaluated the magnetization change ΔM and heat input Q_{in} for several materials and summarized them in Fig. 2 in Ashby-type plots.

We selected only the materials with a transition temperature between 273 K and 373 K, at which water can be used as a heat transfer fluid (Fig. S4 of the supplementary material). We also include the few materials exhibiting a so called "inverse caloric effect," where the magnetization increases upon heating. They are also suitable for thermomagnetic harvesting; just within the cycles illustrated in Fig. 1, the words "apply" and "remove" must be switched. In most TMM systems, the transition temperatures can be tuned by adjusting the composition, which can be used to adapt T_t to the available waste heat. Pure magnetic elements (Fe, Ni, Co) are shown only for comparison, as they have T_t far above the relevant temperature range. The benchmark is the Carnot efficiency $\eta_{carnot} = \Delta T / T_{hot}$, which represents the upper theoretical limit according to
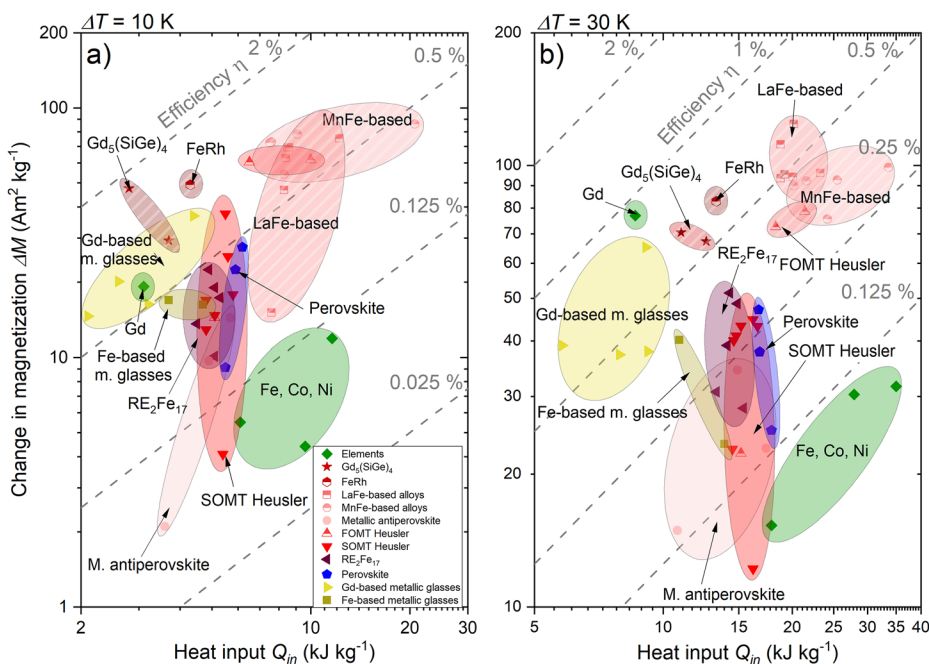

FIG. 2. Evaluating the thermodynamic efficiency η of thermomagnetic materials. To reach high η, a large change in magnetization ΔM is beneficial, as well as a low heat input Q_{in}. The gray dashed lines represent a constant efficiency $\eta = \mu_0 \Delta M H Q_{in}^{-1}$. Accordingly, the most efficient materials are located in the top left corner, where η approaches 2%. Material properties were evaluated for two different temperature spans in Ashby-type plots. (a) At $\Delta T = 10$ K, materials exhibiting a first order transition (half solid symbols) reach the highest efficiencies. (b) At $\Delta T = 30$ K, materials with a second order transition (solid symbols) become competitive. Metallic materials are displayed in shades of red, ceramics in blue, metallic glasses in shades of yellow, and elements in green.

equilibrium thermodynamics. The most efficient TMMs are ones in which a maximum of ΔM is obtained at a minimum Q_{in}: these are found in the top left corner of the Ashby plots. We selected two different values for ΔT: 10 K and 30 K. For the low value of ΔT, materials with the tendency of a first order transition are the most suitable as they exhibit a sharp transition where ΔM changes in a narrow ΔT.

For a large ΔT, materials with a second order transition become competitive, which exhibit a gradual decrease in magnetization during heating. The best TMM can reach an efficiency of about 2%, which is about 60% of the upper limit of η_{carnot} = 3.3% for T_{hot} = 300 K and ΔT = 10 K. Of particular interest is Gd, which was used for several demonstrators and is the benchmark material for magnetocaloric refrigeration. For ΔT = 10 K, we obtain an absolute efficiency of 0.62%, which is quite close to the value of 0.67% obtained by Hsu et al.[39] This good agreement confirms the validity of our approximation method since Hsu et al. obtained their values by numerical integration.

As we will analyze in detail later, the high values for efficiency illustrate that even the existing TMM can compete with thermoelectrics. This is quite astonishing since most of the materials summarized here had been developed for magnetocaloric refrigeration, which must convert a large amount of heat during each cycle. For energy harvesting, a new paradigm for materials development is necessary: the TMM should consume Q_{in} as low as possible, and accordingly, one must aim for low heat capacity and latent heat.

D. Power density, specific cost, and economic feasibility

A decisive criterion for which the TMM will be used for real-world applications is its cost effectiveness, which describes the price for each watt of electric power harvested. To probe if the cost effectiveness of the TMM can compete with that of thermoelectrics or even conventional sources of electrical energy, we expand our analysis of thermodynamic efficiency toward power density and specific cost.

The power density P_D describes the power per unit volume that can be harvested by a TMM: $P_D = E_{mag} \cdot f$. High P_D requires high energy per cycle E_M as well as high cycle frequency f. The latter requires fast heat exchange, which, in turn, relies on high thermal conductivity λ and low volumetric specific heat ρc_p, where ρ is the density. We used a one-dimensional lumped capacitance method to derive an analytical formula for f (see Fig. S7 of the supplementary material for details). This method considers irreversible losses by heat exchange of a thermomagnetic plate and identifies f for maximum power. In addition to the material's thermal properties (Fig. S3 of the supplementary material), only the thickness d of the TMM is required. We selected d = 0.5 mm because this thickness is achievable by most bulk-processing routes. Indeed, for the La–Fe–Co–Si materials, plates with this thickness are already available commercially.

To estimate the specific material cost C, we used the current raw-material prices per volume. We did not include the costs of processing and shaping in the present analysis, as these costs depend on the scale of production and are expected to decrease strongly once thermomagnetic harvesting is established. Furthermore, we considered only the TMM and not the periphery required for a complete

thermomagnetic system (hard magnets, soft magnetic yoke, tubing, etc.). Our cost estimates, thus, represent the lower limit. A realistic estimate of the periphery is not possible at the present level of technology readiness, but note that the use of cheap ferrite hard magnets appears possible,[37] whereas magnetocaloric refrigeration requires expensive Nd–Fe–B.

To evaluate the cost effectiveness of the TMM, we calculated the cost index C/P_D, which gives the price in euro required for each Watt of output power (Fig. 3). This allows for a rough comparison with the costs of common power generation, which is quantified by the Levelized Cost Of Electricity (LCOE), which considers the construction, operation, and financing of a power plant during lifetime. Accordingly, the cost index we use for the raw materials is just a fraction of the complete LCOE. The LCOE of present-day power plants ranges from 0.4 € W^{-1} for gas turbines to 4 € W^{-1} for offshore wind plants.[40] Recent calculations of thermoelectric systems propose that it can reach ~11 € W^{-1}.[4] However, these particular calculations assume a temperature difference of 110 K—much more than 30 K, which we used in Fig. 3 to identify the cost-effective TMM. As the
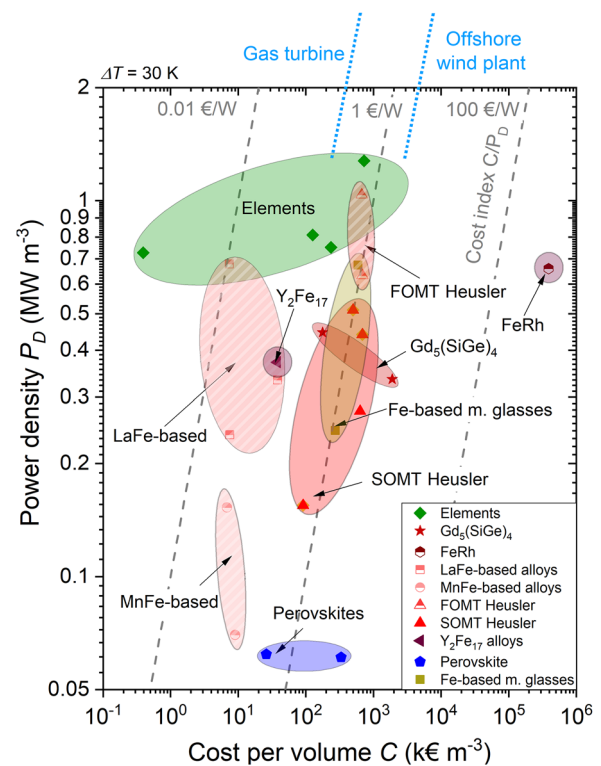

FIG. 3. Identifying the most cost-effective thermomagnetic materials. Ashby-type plot of power density vs cost per volume for ΔT = 30 K. The diagonal gray lines depict the cost index C/P_D, and accordingly, the most cost-effective materials are found in the top left edge. For comparison, the levelized costs of current energy technologies are noted at the top. Though C considers only the cost of the active material and not the periphery (yoke, permanent magnets, processing, etc.), this illustrates that harvesting low grade waste by thermomagnetic materials can become competitive with that by conventional power plants as no additional primary energy is needed.

efficiency of thermoelectrics decreases strongly at a lower temperature difference, in Sec. III G, we will analyze this aspect in more detail.

The pure metals (green), in particular iron, in Fig. 3 reach the lowest cost index but are not suitable due to their low thermodynamic efficiency (Fig. 2). Among the materials with high efficiency, the lowest cost index is obtained for the La–Fe based TMM. Its cost index is more than one order of magnitude lower than the LCOE of present-day power plants. This should leave a sufficient budget for building a complete thermomagnetic system, not least given that waste heat is available for free. We expect that the high cost effectiveness of the TMM will be more decisive for the success of thermomagnetic harvesting than thermodynamic efficiency, which describes only how much waste heat is required.

E. Optimum thermomagnetic materials today and guidelines for future development

The Ashby plots (Figs. 2 and 3) helped us identify the best classes of TMMs that are currently available in terms of their thermodynamic efficiency and cost effectiveness. Here, we focus on the four optimum alloy compositions and discuss their suitability for particular applications. Furthermore, we derive guidelines for improving TMMs further by comparing the different material classes.

The properties of the four most promising TMMs and their particular compositions are summarized in Fig. 4. Gadolinium, which is still the benchmark for magnetocaloric refrigeration,[41] is added as a reference. While the first order $LaFe_{11.8}Si_{1.8}H_1$ exhibits the optimum combination of all properties for bulk applications, $Mn_{1.25}Fe_{0.7}P_{0.5}Si_{0.5}$ has a substantially lower thermal diffusivity, which reduces frequency and, accordingly, power density. The first order Heusler alloys reach the highest power density, but they exhibit a very high specific material cost. Although this cost will hinder bulk application, this is not the case with application in microsystems, for which the material cost is less important than the processing cost. Y_2Fe_{17} is the most promising thermomagnetic material with a second order transition.

To identify guidelines for the optimum TMM, in both Ashby plots, the different material classes are color and symbol coded. TMMs with a first order transition reach higher efficiency at $\Delta T = 10$ K, which we attribute to their steep change in magnetization. Accordingly, some first order materials also achieve an excellent cost index. However, this only holds for La–Fe-based and Mn–Fe-based materials, which both have moderate material costs due to their high content of inexpensive Fe. Furthermore, in both of these material classes, the composition can be used to tune the transformation close to second order.[42,43] By this, one keeps a reasonably steep change in magnetization but avoids the large hysteresis, which often occurs in first order materials and hinders full reversibility.[44] At $\Delta T = 30$ K, materials with a second order transition become competitive; these materials require a larger ΔT and Q_{in} to reach a sufficiently high ΔM. Thus, second order materials are interesting when a large temperature span of waste heat is available.

Crystalline metallic materials can reach higher values of ΔM compared to ceramics as they have a higher magnetization because of a higher density of ferromagnetic elements. Furthermore, ceramics have a low thermal conductivity as compared to metals because
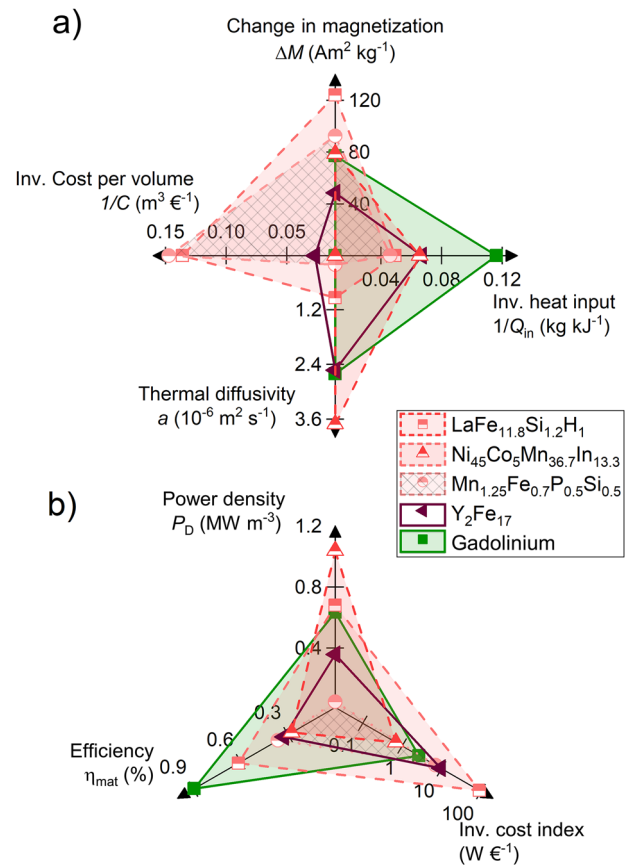

FIG. 4. The four most promising thermomagnetic materials. (a) Physical and economic properties. (b) Thermomagnetic properties. The radar charts are generated by using the best composition for each material class for $\Delta T = 30$ K. Gd is depicted as a reference.

of the absence of free electrons in the former, and thus, their power density is low. Metallic glasses typically have even lower ΔM because of their broad second order transition, but the equally reduced Q_{in} results in a competitive thermodynamic efficiency. However, additional alloying is required to enable the formation of glass, which makes glasses expensive. Thus, we propose that the future work will focus on crystalline metallic materials with a high content of iron when searching for a better TMM. A more detailed evaluation of each material system is provided in Table S2 of the supplementary material.

F. Hysteresis in thermomagnetic materials

An additional aspect, which should be considered during material selection, is hysteresis.[45] Hysteresis occurs in first order materials due to the need for nucleation and growth during transition and can be quantified, e.g., by the temperature span ΔT_{hyst} between the heating and the cooling branch. It is a particularly important aspect for magnetocaloric materials and a key reason that hinders the application of materials, which exhibit a hysteresis above several Kelvin. The reason for this is the relatively small adiabatic temperature change

ΔT_{ad} of a few Kelvin in these materials due to the limited magnetic field achievable by permanent magnets. If ΔT_{hyst} approaches or even exceeds ΔT_{ad}, a completely reversible process is not possible, which reduces or even inhibits the magnetocaloric effect. Therefore, already a small hysteresis has a major impact on the performance of magnetocaloric materials. However, for thermomagnetic energy harvesting, this is different, as the applied temperature difference ΔT between hot and cold states is, in general, much higher than ΔT_{ad}. In a simplified picture, ΔT_{hyst} is required as an additional temperature difference to overcome hysteresis. Though this reduces efficiency, using a few additional Kelvin of waste heat allows us to close a thermomagnetic harvesting cycle. Thus, in general, hysteresis is less critical for thermomagnetic materials than for magnetocaloric materials.

Beyond this simplified picture, we investigated the influence of the thermal hysteresis on a La–Fe–Co–Si alloy in detail.[37] This is the same alloy, which we identified as most promising within the present survey. As this alloy is at the border between a first and a second order transition, it exhibits a low hysteresis of 1 K. In our previous analysis, we could show that this hysteresis reduces the flux change (and, thus, the output power) only marginally. For instance, at $\Delta T = 30$ K, the reduction is as low as 1%.

Hysteresis is an extrinsic material property, which strongly depends on the microstructure, and accordingly, several approaches are known to reduce hysteresis by material design[46–48] and minor loops.[49] As our analysis is based on intrinsic material properties and equilibrium thermodynamics, it cannot be incorporated into hysteresis directly. We considered hysteresis in our survey by selecting only materials with a hysteresis up to 10 K, and indeed, most of the materials have a hysteresis below 5 K. We consider this appropriate for Ashby-type diagrams, exhibiting logarithmic axes. For a more detailed material selection on a linear scale, one should consider hysteresis, as described, e.g., in Ref. 37.

G. Identifying the optimum temperature range for thermomagnetic energy harvesting in comparison with thermoelectrics

Our analysis of cost effectiveness reveals that thermomagnetic materials have the potential to be cheaper than thermoelectric materials. In this section, we return to thermodynamic efficiency in order to benchmark the best thermomagnetic and thermoelectric materials with respect to the ideal temperature difference ΔT. Following our previous analysis, La–Fe-based TMMs are most promising for bulk applications. For this benchmark, we selected the particular La–Fe–Co–Si system, as plates are already available commercially (Calorivac C®).[50] This geometry is favorable for most applications, as it enables both guiding the magnetic flux within the plate and a fast perpendicular heat transfer.[37] The hydrogenized La–Fe alloys, which reach slightly higher values, are not available in plate shape. To determine $\eta(T)$ [Eq. (2)], we measured ΔM and Q_{in} in dependency of temperature (Fig. S1 of the supplementary material). Both properties exhibit different dependencies on ΔT. ΔM has a favorable high value just at the transition temperature, as this temperature is defined as the inflection point of the $M(T)$ curve. In contrast to this, Q_{in} increases continuously with increasing ΔT. Accordingly, large temperature differences are unfavorable and the
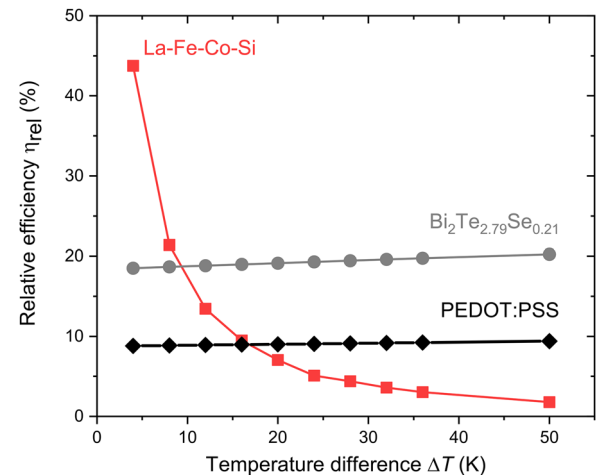

FIG. 5. Efficiency relative to Carnot of TMMs and thermoelectric materials for harvesting low-temperature waste heat. The relative efficiency η_{rel} of the TMM like La–Fe–Co–Si (Calorivac C) increases strongly at low-temperature differences. For comparison, $Bi_2Te_{2.79}Se_{0.21}$ as the most efficient thermoelectric material[51] and PEDOT:PSS[53] as the more sustainable organic material with lower cost are shown. The high efficiency of the TMM is of particular advantage when only temperature differences up to several 10 K are available.

efficiency of thermomagnetic harvesting increases strongly at low ΔT (Fig. 5).

For comparison, we calculate the relative efficiency of thermoelectric materials using $\eta_{rel} = \frac{\eta}{\eta_{Carnot}} = \frac{\sqrt{1+Z\bar{T}}-1}{\sqrt{1+Z\bar{T}}+T_{cold}/T_{hot}}$, where ZT is the unitless figure of merit at the application temperature and $\bar{T}$ is the average temperature of the hot temperature T_{hot} and cold temperature T_{cold}.[51] As with thermomagnetics, this materials efficiency is the upper limit of the system efficiency, which can be significantly lower.[52] We plot η_{rel} for two important thermoelectric materials. $Bi_2Te_{2.79}Se_{0.21}$ is the material reaching the highest values around room temperature.[51] The organic thermoelectric material PEDOT:PSS[53] has lower values, but this material is more suitable for this low-temperature range as it is cheaper and more sustainable.[5] At temperature differences below 10 K, TMMs reach much higher efficiencies than thermoelectric materials, which is a key advantage for several applications. An example of such low grade waste heat is body heat, which makes thermomagnetic microsystems, in particular, suitable to power, e.g., smartwatches.[54] This case illustrates the urgent need for highly efficient energy materials for the case when only a low-temperature difference is available. A second example is geothermal energy, which uses a larger temperature span to turn off grid devices. To expand the temperature range for thermomagnetic energy harvesting, one can use a series of TMMs with increasing transition temperatures. In this series, each particular TMM just takes its optimum ΔT from the heat source and leaves a colder sink for its neighboring TMM, having a lower transition temperature. This approach is equivalent to the "active regenerator" approach used for magnetocaloric refrigeration to reach a higher cooling span.[55] Though the application of this approach for energy harvesting had been proposed in the past,[56] it has not yet been realized experimentally.

IV. CONCLUSION

Thermomagnetic materials (TMMs) enable the conversion of low-temperature waste heat to electricity by the change in magnetization with temperature. Though their implementations in harvesting systems such as motors, oscillators, and generators differ with respect to the mechanical motion, the TMM always follows the same thermodynamic cycle. This allows for a universal evaluation of the TMM from its material properties. We present two Ashby-type charts—one for thermodynamic efficiency and another for cost effectiveness—which serve as figures of merit for TMMs. This materials library enables scientists and engineers to select the optimum thermomagnetic material for their demand.

We identify several TMMs that have the potential to compete with thermoelectric materials for temperature differences below 10 K with respect to efficiency. This is a decisive advantage because the largest amount of waste heat is available just above room temperature. Furthermore, our analysis reveals that the price per watt of the best TMM is more than one order of magnitude lower than that of established power technologies and thermoelectrics. This price is competitive enough to make it economically feasible to realize a complete thermomagnetic system.

SUPPLEMENTARY MATERIAL

See the supplementary material for additional information on material data of relevant thermomagnetic materials (Table T1), characterization of thermomagnetic materials exemplarily for a La–Fe–Co–Si material (Fig. S1), precise determination of magnetic energy during a thermomagnetic cycle (Fig. S2), thermal properties of thermomagnetic materials (Fig. S3), magnetization change and transition temperature of thermomagnetic materials (Fig. S4), Ashby-type plot for high power per mass function (Fig. S5), Ashby-type plot for high efficiency and power (Fig. S6), comparison and evaluation of different material systems (Table T2), and calculation of the cycle frequency (Fig. S7).

AUTHORS' CONTRIBUTIONS

D.D. compared the different TMMs and wrote the first version of this paper. A.W. contributed to the extrinsic properties and comparison with magnetocaloric materials. K.N. supervised the thesis of D.D. and contributed to the comparison with thermoelectric materials. S.F. suggested to make this analysis and wrote the second version of this paper. All authors contributed to the final version.

ACKNOWLEDGMENTS

DATA AVAILABILITY

The data that support the findings of this study are available within this article and its supplementary material or are available from the corresponding author upon reasonable request.

REFERENCES

[1] D. P. Van Vuuren, D. L. Bijl, P. Bogaart, E. Stehfest, H. Biemans, S. C. Dekker, J. C. Doelman, D. E. H. J. Gernaat, and M. Harmsen, "Integrated scenarios to support analysis of the food-energy-water nexus," Nat. Sustainability **2**, 1132–1141 (2019).

[2] C. Forman, I. K. Muritala, R. Pardemann, and B. Meyer, "Estimating the global waste heat potential," Renewable Sustainable Energy Rev. **57**, 1568–1579 (2016).

[3] G. Schierning, "Bring on the heat," Nat. Energy **3**, 92–93 (2018).

[4] M. Araiz, Á. Casi, L. Catalán, Á. Martínez, and D. Astrain, "Prospects of waste-heat recovery from a real industry using thermoelectric generators: Economic and power output analysis," Energy Convers. Manage. **205**, 112376 (2020).

[5] B. Russ, A. Glaudell, J. J. Urban, M. L. Chabinyc, and R. A. Segalman, "Organic thermoelectric materials for energy harvesting and temperature control," Nat. Rev. Mater. **1**, 16050 (2016).

[6] V. K. Pecharsky and K. A. Gschneidner, Jr., "Giant magnetocaloric effect in $Gd_5(Si_2Ge_2)$," Phys. Rev. Lett. **78**, 4494–4497 (1997).

[7] J. Liu, T. Gottschall, K. P. Skokov, J. D. Moore, and O. Gutfleisch, "Giant magnetocaloric effect driven by structural transitions," Nat. Mater. **11**, 620 (2012).

[8] A. Kitanovski, J. Tušek, U. Tomc, U. Plaznik, M. Ožbolt, and A. Poredoš, "The thermodynamics of magnetocaloric energy conversion," in *Magnetocaloric Energy Conversion: From Theory to Applications* (Springer International Publishing, Cham, Switzerland, 2015), pp. 1–21.

[9] A. Kitanovski and P. W. Egolf, "Innovative ideas for future research on magnetocaloric technologies," Int. J. Refrig. **33**, 449–464 (2010).

[10] V. Franco, J. S. Blázquez, J. J. Ipus, J. Y. Law, L. M. Moreno-Ramírez, and A. Conde, "Magnetocaloric effect: From materials research to refrigeration devices," Prog. Mater Sci. **93**, 112–232 (2018).

[11] N. Tesla, "Thermo-magnetic motor," U.S. patent 396121A (Jan. 15 1889).

[12] N. Tesla, "Pyromagneto-electric generator," U.S. patent 428057A (May 13 1890).

[13] J. Stefan, "Ueber thermomagnetische motoren," Ann. Phys. **274**, 427–440 (1889).

[14] T. A. Edison, "Pyromagnetic motor," U.S. patent 380100A (Mar. 27 1888).

[15] T. A. Edison, "Pyromagnetic generator," U.S. patent 476983A (June 14 1892).

[16] V. Srivastava, Y. Song, K. Bhatti, and R. D. James, "The direct conversion of heat to electricity using multiferroic alloys," Adv. Energy Mater. **1**, 97–104 (2011).

[17] R. Bozorth, *Ferromagnetism* (Wiley, Hoboken, NJ, USA, 1993).

[18] B. Yu, M. Liu, P. W. Egolf, and A. Kitanovski, "A review of magnetic refrigerator and heat pump prototypes built before the year 2010," Int. J. Refrig. **33**, 1029–1060 (2010).

[19] R. A. Kishore and S. Priya, "A review on design and performance of thermomagnetic devices," Renewable Sustainable Energy Rev. **81**, 33–44 (2018).

[20] A. Kitanovski, "Energy applications of magnetocaloric materials," Adv. Energy Mater. **10**, 1903741 (2020).

[21] F. Brailsford, "Theory of a ferromagnetic heat engine," Proc. Inst. Electr. Eng. **111**, 1602–1606 (1964).

[22] W. A. Steyert, "Stirling-cycle rotating magnetic refrigerators and heat engines for use near room temperature," J. Appl. Phys. **49**, 1216 (1978).

[23] H. Toftlund, "A rotary Curie point magnetic engine: A simple demonstration of a Carnot-cycle device," Am. J. Physiol. **55**, 48–49 (1987).

[24] Swiss Blue Energy AG, "Der neue geniale beitrag zum energiewandel," http://www.swiss-blue-energy.ch/en/index.html, 2020.

[25] M. Gueltig, F. Wendler, H. Ossmer, M. Ohtsuka, H. Miki, T. Takagi, and M. Kohl, "High-performance thermomagnetic generators based on heusler alloy films," Adv. Energy Mater. **7**, 1601879 (2017).

[26] J. Chun, H.-C. Song, M.-G. Kang, H. B. Kang, R. A. Kishore, and S. Priya, "Thermo-magneto-electric generator arrays for active heat recovery system," Sci. Rep. **7**, 41383 (2017).

[27] T. Chung, D. Lee, M. Ujihara, and G. P. Carman, "Design, simulation, and fabrication of a novel vibration-based magnetic energy harvesting device," in *Transducers 2007 - 2007 International Solid-State Sensors, Actuators and Microsystems Conference* (IEEE, 2007), pp. 867–870.

[28] M. Ujihara, G. P. Carman, and D. G. Lee, "Thermal energy harvesting device using ferromagnetic materials," Appl. Phys. Lett. **91**, 093508 (2007).

[29]S. Moss, A. Barry, I. Powlesland, S. Galea, and G. P. Carman, "A low profile vibro-impacting energy harvester with symmetrical stops," Appl. Phys. Lett. **97**, 234101 (2010).

[30]K. Deepak, V. B. Varma, G. Prasanna, and R. V. Ramanujan, "Hybrid thermomagnetic oscillator for cooling and direct waste heat conversion to electricity," Appl. Energy **233-234**, 312–320 (2019).

[31]L. Brillouin and H. Iskenderian, "Thermomagnetic generator," Electr. Commun. **25**, 300–311 (1948).

[32]J. F. Elliott, "Thermomagnetic generator," J. Appl. Phys. **30**, 1774–1777 (1959).

[33]H. E. Stauss, "Efficiency of thermomagnetic generator," J. Appl. Phys. **30**, 1622–1623 (1959).

[34]L. D. Kirol and J. I. Mills, "Numerical analysis of thermomagnetic generators," J. Appl. Phys. **56**, 824–828 (1984).

[35]D. Solomon, "Improving the performance of a thermomagnetic generator by cycling the magnetic field," J. Appl. Phys. **63**, 915–921 (1988).

[36]T. Christiaanse and E. Brück, "Proof-of-concept static thermomagnetic generator experimental device," Metall. Mater. Trans. E **1**, 36–40 (2013).

[37]A. Waske, D. Dzekan, K. Sellschopp, D. Berger, A. Stork, K. Nielsch, and S. Fähler, "Energy harvesting near room temperature using a thermomagnetic generator with a pretzel-like magnetic flux topology," Nat. Energy **4**, 68–74 (2019).

[38]A. Czernuszewicz, J. Kaleta, M. Królewicz, D. Lewandowski, R. Mech, and P. Wiewiórski, "A test stand to study the possibility of using magnetocaloric materials for refrigerators," Int. J. Refrig. **37**, 72–77 (2014).

[39]C.-J. Hsu, S. M. Sandoval, K. P. Wetzlar, and G. P. Carman, "Thermomagnetic conversion efficiencies for ferromagnetic materials," J. Appl. Phys. **110**, 123923 (2011).

[40]Fraunhofer ISE, "Levelized cost of electricity renewable energy technologies," https://www.ise.fraunhofer.de/content/dam/ise/en/documents/publications/studies/EN2018_Fraunhofer-ISE_LCOE_Renewable_Energy_Technologies.pdf, 2019.

[41]T. Gottschall, K. P. Skokov, M. Fries, A. Taubel, I. Radulov, F. Scheibel, D. Benke, S. Riegg, and O. Gutfleisch, "Making a cool choice: The materials library of magnetic refrigeration," Adv. Energy Mater. **9**, 1901322 (2019).

[42]E. Lovell, L. Ghivelder, A. Nicotina, J. Turcaud, M. Bratko, A. D. Caplin, V. Basso, A. Barcza, M. Katter, and L. F. Cohen, "Low-temperature specific heat in hydrogenated and Mn-doped La(Fe, Si)$_{13}$," Phys. Rev. B **94**, 134405 (2016).

[43]N. Van Thang, N. Van Dijk, and E. Brück, "Tuneable giant magnetocaloric effect in (Mn,Fe)(2)(P,Si) materials by Co-B and Ni-B Co-doping," Materials **10**, 14 (2016).

[44]L. F. Cohen, "Contributions to hysteresis in magnetocaloric materials," Phys. Status Solidi B **255**, 1700317 (2018).

[45]O. Gutfleisch, T. Gottschall, M. Fries, D. Benke, I. Radulov, K. P. Skokov, H. Wende, M. Gruner, M. Acet, P. Entel, and M. Farle, "Mastering hysteresis in magnetocaloric materials," Philos. Trans. R. Soc. A **374**, 20150308 (2014).

[46]F. Scheibel, T. Gottschall, A. Taubel, M. Fries, K. P. Skokov, A. Terwey, W. Keune, K. Ollefs, H. Wende, M. Farle, M. Acet, O. Gutfleisch, and M. E. Gruner, "Hysteresis design of magnetocaloric materials – from basic mechanism to application," Energy Technol. **6**, 1397 (2018).

[47]Y. Zhang, J. Wang, X. Ke, T. Chang, F. Tian, C. Zhou, S. Yang, M. Fang, K. Cao, Y.-S. Chen, Z. Sun, W. Guan, X. Song, and X. Ren, "Zero-thermal-hysteresis magnetocaloric effect induced by magnetic transition at a morphotropic phase boundary in Heusler Ni$_{50}$Mn$_{36}$Sb$_{14-x}$In$_x$," Phys. Chem. Chem. Phys. **20**, 18484–18490 (2018).

[48]F. Guillou, G. Porcari, H. Yibole, N. van Dijk, and E. Brück, "Taming the first-order transition in giant magnetocaloric materials," Adv. Mater. **26**, 2671–2675 (2014).

[49]A. Diestel, R. Niemann, B. Schleicher, K. Nielsch, and S. Fähler, "Reducing hysteresis losses by heating minor loops in magnetocaloric Ni-Mn-Ga-Co," Energy Technol. **6**, 1463 (2018).

[50]VACVACUUMSCHMELZE, "Advanced materials - the key to progress vacuumschmelze," https://vacuumschmelze.com/products/Further-Technologies/Magnetocaloric-Material–CALORIVAC, June 5, 2019, Vacuumschmelze, 2015.

[51]L. Yang, Z.-G. Chen, M. S. Dargusch, and J. Zou, "High performance thermoelectric materials: Progress and their applications," Adv. Energy Mater. **8**, 1701797 (2018).

[52]P. Jood, M. Ohta, A. Yamamoto, and M. G. Kanatzidis, "Excessivley doped PbTe with Ge-induced nanostructures enables high-efficiency thermoelectric modules," Joule **2**, 1339–1355 (2018).

[53]G.-H. Kim, L. Shao, K. Zhang, and K. P. Pipe, "Engineered doping of organic semiconductors for enhanced thermoelectric efficiency," Nat. Mater. **12**, 719–723 (2013).

[54]J. A. Paradiso and T. Starner, "Energy scavenging for mobile and wireless electronics," IEEE Pervasive Comput. **4**, 18–27 (2005).

[55]A. Rowe and A. Tura, "Experimental investigation of a three-material layered active magnetic regenerator," Int. J. Refrig. **29**, 1286–1293 (2006).

[56]G. Russberg and S. Thorburn, "Arrangement and method for thermomagnetic power generation," U.S. patent WO2010/139538A1 (Dec. 9, 2010).